



Norwegian University of  
Science and Technology

# The Effect of Blockage on High Reynolds Number Flow over a semi- circular Obstacle

**Stig Sund**

Master of Science in Product Design and Manufacturing

Submission date: June 2010

Supervisor: Lars Sætran, EPT



# Problem Description

In large scale, high Reynolds number flows over bluff bodies the flow characteristics are influenced by the geometry of the bluff body. Examples are pipelines lying on the sea floor and wind flow over hills. In the first case the separation of the flow from the surface of the body is important for both static and dynamic drag characteristics on the body. In the second case the shape of the body influences the developing flow over the body surface, which will have effects on the profiles of mean wind speed and turbulence. Such effects are important for choosing effective sites for wind turbines.

Flow phenomena as described above are often investigated using wind tunnels where one will have to both consider the scaling problem (full scale versus laboratory scale) and the blockage problem in cases where the experiment is performed in test sections constrained by walls.

In this project both the scaling and blockage problems shall be addressed theoretically/ experimentally using wind tunnels and instrumentation that are available at the department.

Assignment given: 18. January 2010  
Supervisor: Lars Sætran, EPT



EPT-M-2010-63

**MASTER THESIS**

for

Stud.techn. Stig Sund  
Spring 2010

*Scaling characteristics of flow over bluff bodies*

*Skalering av strømming over butte legemer*

In large scale, high Reynolds number flows over bluff bodies the flow characteristics are influenced by the geometry of the bluff body. Examples are pipelines lying on the sea floor and wind flow over hills. In the first case the separation of the flow from the surface of the body are important for both static and dynamic drag characteristics on the body. In the second case the shape of the body influences on the developing flow over the body surface, which will have effects on the profiles of mean wind speed and turbulence. Such effects are important for choosing effective sites for wind turbines.

Flow phenomenon as described above are often investigated using wind tunnels where one will have to both consider the scaling problem (full scale versus laboratory scale) and the blockage problem in cases where the experiment is performed in test sections constrained by walls.

In this project both the scaling and blockage problems shall be addressed theoretically/experimentally using wind tunnels and instrumentation that are available at the department.

-- ” --

Within 14 days of receiving the written text on the diploma thesis, the candidate shall submit a research plan for his project to the department.

When the thesis is evaluated, emphasis is put on processing of the results, and that they are presented in tabular and/or graphic form in a clear manner, and that they are analyzed carefully.

The thesis should be formulated as a research report with summary both in English and Norwegian, conclusion, literature references, table of contents etc. During the preparation of the text, the candidate should make an effort to produce a well-structured and easily readable report. In order to ease the evaluation of the thesis, it is important that the cross-references are correct. In the making of the report, strong emphasis should be placed on both a thorough discussion of the results and an orderly presentation.

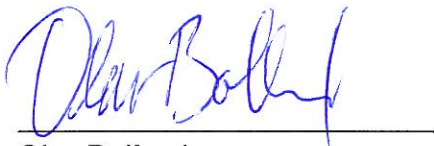
The candidate is requested to initiate and keep close contact with his/her academic supervisor(s) throughout the working period. The candidate must follow the rules and regulations of NTNU as well as passive directions given by the Department of Energy and Process Engineering.

Pursuant to "Regulations concerning the supplementary provisions to the technology study program/Master of Science" at NTNU §20, the Department reserves the permission to utilize all the results and data for teaching and research purposes as well as in future publications.

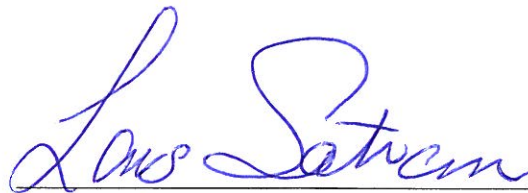
One – 1 complete original of the thesis shall be submitted to the authority that handed out the set subject. (A short summary including the author's name and the title of the thesis should also be submitted, for use as reference in journals (max. 1 page with double spacing)).

Two – 2 – copies of the thesis shall be submitted to the Department. Upon request, additional copies shall be submitted directly to research advisors/companies. A CD-ROM (Word format or corresponding) containing the thesis, and including the short summary, must also be submitted to the Department of Energy and Process Engineering

Department of Energy and Process Engineering, 12. January 2010



Olav Bolland  
Department Manager



Lars Sætran  
Academic Supervisor







# The Effect of Blockage on High Reynolds Number Flow over a semi-circular Obstacle

Stig Sund, *Stud.Techn.*,  
Norwegian University of Science and Technology

**Abstract**—In order to map the effects of blockage and aspect ratio, pressure distributions were measured around four different floor-mounted semi-circular cylinders in nominally two-dimensional flow. Diameters ranged from 0.05 m to 0.30 m for  $0.3 \cdot 10^5 \leq Re \leq 3.5 \cdot 10^5$ . No significant blockage effects were found for  $B = 0.05$ . It was shown that by using  $U_b$  as the reference velocity, blockage and aspect ratio effects could be partially counteracted. The use of  $U_b$  was identified to be especially efficient in correcting  $c_{pb}$ , but led to a larger variation of the minimum pressure coefficient with  $Re$ , for a given blockage ratio. Results also indicate that blockage is the governing factor of  $c_{pb}$  for  $L/D > 10$ , while the aspect ratio has the largest influence below this threshold. Separation bubbles occur in a manner similar to that of circular cylinders. The results do, however, indicate that the progression from laminar separation to purely turbulent separation may be accelerated by increased blockage. Further, the speed up over the cylinder was found to be approximately constant for a given blockage, and proportional to  $B^2$ .

## I. INTRODUCTION

This article describes a series of experiments carried out to investigate the effects of blockage on the flow over a semi-circular floor-mounted cylinder in a rectangular wind tunnel.

As the need for subsea pipelines to transport oil and gas started to grow rapidly from the 1970s, a new focus on understanding the mechanisms at work throughout the life-span of such a pipe arose. Important early work on understanding the wake of, and force on, a cylinder near, or on, a plane surface was performed by Bearman and Zdravkovich [1][2]. However, some pipelines are also partially buried either at installation, by natural filling of the pipe trench, or as a result of self-burial during its life-span [3]. Several experiments have been performed on partially buried cylinders exposed to a steady current [4][5], or waves superimposed on a steady current [6][7][8][9][10][11]. However, most of the data available is the result of laboratory experiments; bringing with it uncertainty about the validity of the experiment, as experimental effect may influence the results.

This article aims to gain more knowledge about the effects encountered when investigating the flow

over a half-buried pipeline, of increasing size, in a tunnel. An attempt will be made to describe the effects of the blockage ratio,  $B$ , and the aspect ratio,  $L/D$ , on the overall properties of the flow.

In addition to the main focus of this investigation, other areas of application may also benefit from the results. Investigations of flow over hills are also known to utilize the simple geometry of the semi-circular floor-mounted cylinder to perform controlled wind tunnel experiments [12]. Furthermore, the case of flow through a channel with a pronounced blockage has in recent studies found a new area of application, as a simple analogue for an obstruction in an arterial passage [13]. Further it has been used to investigate flow over, and resulting forces on, contemporary [14][15], as well as historical [16], structures.

When studying the case of a circular cylinder in nominally free flow, the free flow velocity,  $U_\infty$ , is used as the reference velocity in dimensionless properties such as  $Re$ ,  $C_D$ ,  $C_L$ ,  $c_p$  and  $c_{pb}$ .

In the study of pipelines and partially buried pipelines, however, some investigations [6][4] use  $U_t$ , the flow velocity just above the top of the cylinder, instead of  $U_\infty$ , as the reference velocity. For flows with a strong boundary layer, use of the former definition may be practical, as  $U_t$  is a direct result of the cylinders influence on the flow. In a situation with a strong incoming boundary layer,  $U_t$  would by this reasoning in practice summarize the incoming flow condition. Consequently providing a more complete picture of the flow around the cylinder.

Another possible reference velocity that could be used is the velocity of the flow between the top of the cylinder and the wind tunnel roof. Utilizing this velocity, defined as bulk flow velocity,  $U_b$ , may be advantageous as it is a result of the constricted flow area, and it is believed that it may counteract the influence blockage to a certain extent.

This article will present and discuss two cases: the cases where  $U_\infty$  and  $U_b$  are used as reference velocities. From now on the use of  $U_\infty$  as the reference velocity will be referred to as method (I),

or just (I), while the use of  $U_b$  will be referred to as method (II), or just (II). The hope is that method (II) will provide an alternative perspective in the analysis, thus providing a good basis of comparison to method (I).

The analysis of the results, Section IV, will aim to describe the mechanisms of the flow around the half-buried cylinders. Where comparable data for semi-circular cylinders is not available, insufficient or ambiguous, flow around circular cylinders in free flow, or close to plane surfaces, will be used in an effort to explain the observed phenomena.

It is possible to divide the effect of blockage into two parts [25]; the *solid blockage* which is the direct influence, i.e. the acceleration of the flow due to the cylinder, and the *wake blockage*, which is the restriction of natural wake development. These definitions will be used when they are helpful for the analysis.

Wong (1981) [16] performed an investigation of the flow over barrel vaults with an experimental setup similar that in the current investigation. He found that the variation of  $C_D$  is much the same as that for a circular cylinder, and observed a minimum  $C_D$  for  $Re \approx 10^5$ .  $C_D$ .

Weidman (1968) [25] found that as the wake behind a circular cylinder narrows,  $c_{pb}$  increases. With a decreased initial size of the wake, and thus an increased value of  $c_{pb}$ , the wake blockage will not be as dominant. The same behavior is expected to be found in the current investigation.

Based on previous results [15][16]  $c_{pb}$  is expected to have a value of approximately 0.6.  $C_D$  and  $C_L$  have been found to attain values of 0.26 and 0.63 [15], respectively.

West and Apelt 1982 [26] investigated the influence of blockage and aspect ratio separately. Their investigation concluded that an increase in blockage and a decrease in aspect ratio both have similar effect on  $C_D$  and  $c_{pb}$ .

For circular cylinders theory and reality both indicate an initial  $c_p$  value of  $\approx 1$ . In the case of floor-mounted semi-circular cylinder potential theory still predicts an initial  $c_p$  of 1, but it has been shown through experiments that this value should be expected to be  $\approx 0.5$  [14][15][16][27].

## II. EXPERIMENTAL SETUP & PROCEDURE

The experiments were performed in a closed circuit wind tunnel at NTNU<sup>1</sup>, with a fixed test section of 1 x 0.5 m, capable producing flow

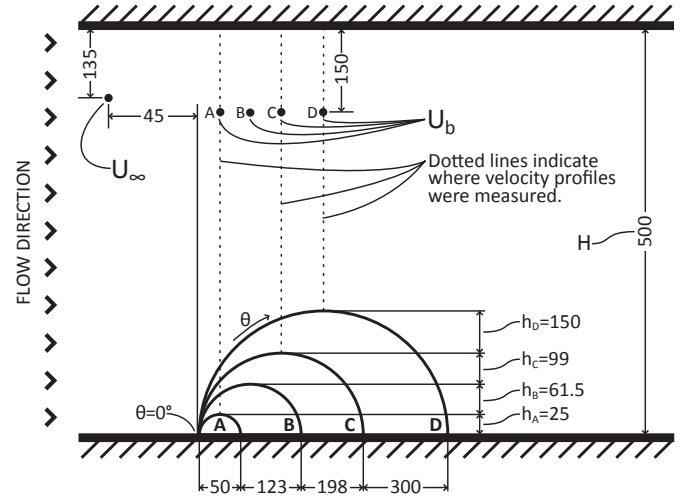


Fig. 1. Schematic of the setup. Note that all measurements are given in mm and that the measurements are not to scale.

velocities up to 30 m/s. The turbulence intensity,  $I_u$ , has been measured to be in the range of 0.31 to 0.38, depending on the wind tunnel velocity<sup>2</sup> [17].

Four 1 m long cylinders with diameters of 0.050 m, 0.123 m, 0.198 m and 0.30 m were divided into two equal parts in the axial direction. For the wind tunnel used this correspond to aspect ratios  $L/D$  of 20, 8.13, 5.05 and 3.33, and blockage ratios  $B$  of 5%, 12.3%, 19.8% and 30%, respectively.

One half of each cylinder was discarded, the other half was fitted with 1 mm diameter pressure taps. The first pressure tap of each cylinder was located at the mid-span, 0.5 m from either wind tunnel wall, 5 mm above the floor of the wind tunnel. Remaining pressure taps were placed with equal spacing in the circumferential direction, directly downstream from the first, see Table I for details.

The half cylinders will be referred to as cylinders for the remainder of this article.

In order to achieve nominally two-dimensional flow conditions, the cylinders spanned the whole width of the wind tunnel, and any unwanted openings between the wind tunnel and the cylinders were sealed. Covering all gaps between the wind tunnel floor and the circular cylinders also helps simulate an impermeable seabed, as used in several earlier investigations [4][6][9].

The cylinders with diameters 0.050 m, 0.123 m and 0.30 m were made of PVC<sup>3</sup>, the remaining cylinder was made of plexiglass<sup>4</sup>. To ensure comparable results, and to provide a certain roughness

<sup>2</sup> $\bar{U} = 15.7$  m/s,  $I_u = 0.38$ ;  $\bar{U} = 22.5$  m/s,  $I_u = 0.32$ ;  $\bar{U} = 25.1$  m/s,  $I_u = 0.33$ ;  $\bar{U} = 28.3$  m/s,  $I_u = 0.31$ ;  $\bar{U} = 32.5$  m/s,  $I_u = 0.34$ .

<sup>3</sup>Polyvinyl chloride

<sup>4</sup>PMMA, Poly(methyl methacrylate)

<sup>1</sup>Norwegian University of Science and Technology, NO-7491 Trondheim, NORWAY

TABLE I

DATA FOR THE CYLINDERS USED IN THE EXPERIMENTS. FOR THE REMAINDER OF THIS ARTICLE EACH CYLINDER SETUP WILL BE REFERRED TO BY THE LETTER ASSIGNED IN THE FIRST COLUMN OF THIS TABLE.

Setup	$D$	Number of pressure taps	Pressure tap spacing	
			[°]	[mm]
A	0.050	10	18°	7.85
B	0.123	19	9°	9.74
C	0.198	24	7.2°	11.88
D	0.300	30	6°	16.44

surface, all the cylinders were given the same finish by polishing with P220 grit sandpaper.

The free stream velocity,  $U_\infty$ , was measured approximately 80 mm upstream of the cylinders leading edge, 135 mm from the wind tunnel roof and 200 mm from the wind tunnel wall. The bulk flow velocity,  $U_b$ , as defined in Section III, was measured 150 mm below the wind tunnel roof and directly above the mid-span of the cylinders.

A seabed current velocity of 0.5 m/s was assumed based on the Metocean Design Criteria for the northern North Sea [18], this velocity was then used to determine a suitable  $Re$ -range for the experiments. For a sea-water temperature of 0°C, this corresponds to  $Re$  of  $0.14 \cdot 10^5$ ,  $0.34 \cdot 10^5$ ,  $0.54 \cdot 10^5$  and  $0.82 \cdot 10^5$ , for Setup A/B/C/D respectively.<sup>5,6</sup> It is, however, important to remember that at typical subsea gas pipeline, which is considered large diameter piping, has a diameter of about 0.75 m, while mid-sized pipelines are about 0.35 m–0.70 m in diameter [19]. Thus, many mid-sized and large pipelines will experience a flow with  $Re$  well above the range that the current setup is capable of producing. However, this is also the case for many studies of flow around half-buried pipelines, which this investigation is meant to be a supplement for.

A range of Reynolds numbers,  $Re$ , similar to the expected  $Re$  values at seabed conditions were chosen. Due to restrictions of the experimental equipment, not all of the Reynolds numbers could be achieved for all the cylinders. Table II offers an overview of the Reynolds numbers used for each cylinder.

For every Reynolds number and setup, several time-series measurements were performed in the wake with a hot-wire anemometer, to determine whether or not regular vortex shedding occurred.

<sup>5</sup>For a sea-water temperature of 20°C, this corresponds to  $Re$  of  $0.24 \cdot 10^5$ ,  $0.57 \cdot 10^5$ ,  $0.94 \cdot 10^5$  and  $1.43 \cdot 10^5$ , for Setup A/B/C/D respectively.

<sup>6</sup>Note that the kinematic viscosity used is that for atmospheric pressure.

TABLE II

OVERVIEW OF THE REYNOLDS NUMBERS USED IN THE EXPERIMENTS FOR EACH CYLINDER. NOTE THAT FOR A GIVEN CYLINDER, THE REYNOLDS NUMBER LISTED HERE IS ONLY APPROXIMATE.

$Re$	Cylinder diameter, $D$			
	0.05	0.123	0.198	0.300
$0.3 \cdot 10^5$	•	•	•	-
$0.4 \cdot 10^5$	•	•	•	-
$0.5 \cdot 10^5$	•	•	•	•
$0.6 \cdot 10^5$	•	•	•	-
$0.7 \cdot 10^5$	•	•	•	-
$0.9 \cdot 10^5$	•	•	•	•
$1.1 \cdot 10^5$	-	•	•	•
$1.5 \cdot 10^5$	-	•	•	•
$2.0 \cdot 10^5$	-	-	•	•
$2.5 \cdot 10^5$	-	-	•	•
$3.0 \cdot 10^5$	-	-	-	•
$3.5 \cdot 10^5$	-	-	-	•

The pressure distribution around the cylinder was obtained by averaging three 10 second mean measurements for each pressure tap. These three measurements were not taken subsequently, but rather as parts of three complete series, spreading them in time. This was done in order to obtain a better average of the flow over time, reducing the chance of capturing transient effects in the measurements. A settling period of 10 seconds was enforced to ensure settling of the pressure after changing pressure taps.

For all *real* flow situations, a boundary layer will be present to some extent. Since the size of the boundary layer relative to the obstacle will depend on a range of factors, it was decided to minimize the boundary layer in order to obtain more general results. To minimize the size of the incoming boundary layer created by the wind tunnel floor, the cylinders were mounted as close as possible to the beginning of the test-section.

Flow velocity profiles were measured between the top of each cylinder and the roof in the center of the wind tunnel for selected  $Re$ . Measurements for comparable  $U_\infty$  were also performed without cylinders installed to establish a baseline. A settling period of 10 seconds was enforced to ensure settling of the pressure after a change in measurement height.

### III. RESULTS

#### A. Pressure distribution

To provide a theoretical point of reference, the potential flow theory solution for the pressure

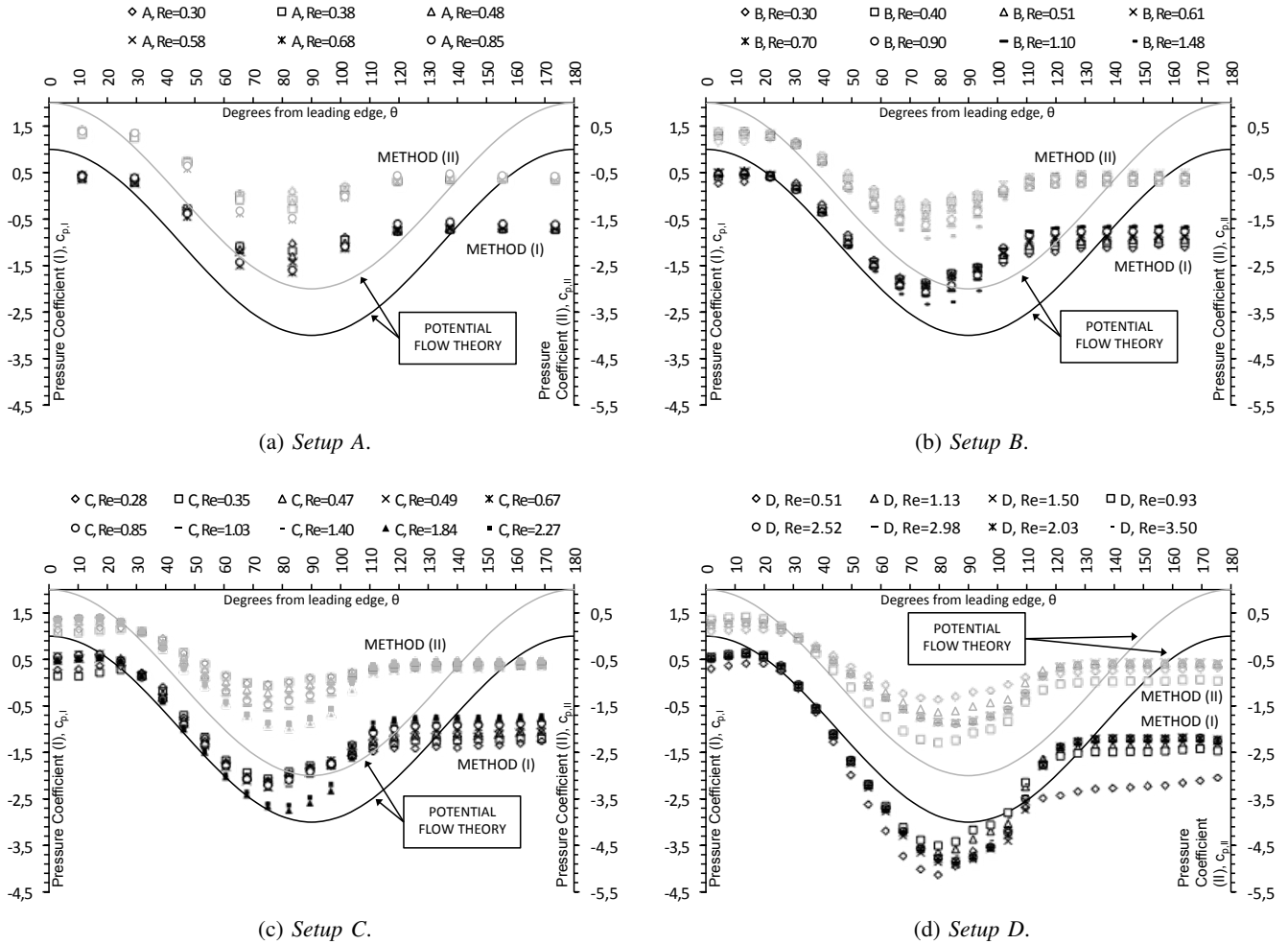


Fig. 2. Pressure coefficient,  $c_p$ , for Setup A/B/C/D. Black markers and black solid lines are for method (I), grey markers and grey solid lines are for method (II). Black and grey relates to the left and right vertical axes, respectively. The solid lines are the  $c_p$  distribution given by potential theory. Note that the vertical axes for a given setup are only shifted vertically, and *not* stretched, in order to keep the shapes of (I) and (II) comparable. Also note that the Reynolds numbers are given as  $Re \cdot 10^{-5}$ .

coefficient for flow around a semi-circular floor mounted cylinder, Eq. (1), is also presented for each case in Fig. 2.

$$c_p = 1 - 4 \cdot \sin^2(\theta) \quad (1)$$

The pressure distribution curves presented in Fig. 2 depicts the pressure coefficient,  $c_p$ , over the span of the cylinder, from  $\theta_a \approx 0^\circ$  at the leading edge to  $\theta_a \approx 180^\circ$  at the trailing edge.<sup>7</sup> For each setup  $c_p$  has been calculated by method (I), represented by black markers, and by method (II), represented by corresponding grey markers.

Setup A show only small differences between method (I) and (II), with the latter yielding slightly less negative values for  $c_{pb}$ . The peripheral measurements collapse marginally better along the same line, but no discernible differences may be observed elsewhere.

<sup>7</sup>The first pressure tap on each cylinder is located 5 mm above the floor of the wind-tunnel, see Section II. The pressure distributions presented do account for the initial value of  $\theta_a$  this implies.

Setup B/C exhibit the same behavior as Setup A close to the leading edge and in the wake region, only more pronounced. The differences between method (I) and method (II) are especially large for the base pressure, which for Setup B has a spread for method (II) that is less than half of that found for method (I). In Setup C, the base pressure collapses almost entirely to the same line for method (II), and has a spread that is only about a third of that for method (I). For the middle of the curve, however, the spread increases similarly for both setups in (II). See Section III-B for further presentation of the base pressure.

It is obvious, and expected, that the theoretical solution does not offer an accurate description of  $c_p$ , but there are certain similarities, and the theoretical solution is an excellent reference for comparison in Fig. 2.

For method (I), each setup follows the trend of the theoretical solution for part of the cylinder span. It is, however, interesting to see that the

agreement between the theoretical and the measured distribution of  $c_p$  increases with increasing blockage for *Setup A/B/C*, the latter exhibits nearly identical values at the largest  $Re$  for  $20^\circ \leq \theta_a \leq 70^\circ$ . In the case of *Setup D* for  $20^\circ \leq \theta_a \leq 70^\circ$ , the slope of the measured  $c_p$  is now steeper than that of the theoretical solution. This is in agreement with the general trend of increased blockage increasing the negative slope for  $c_p$  on the upstream side of the cylinders.

Values for  $c_p$  calculated by method (II) are in less agreement with theory. For the  $\theta_a$ -range with generally good compliance in method (I), it is now observed that that overall slope of the measured  $c_p$  is less negative and that the distance between theory and reality has increased. However, as  $B$  increases, the slope becomes progressively more negative, the result being that for  $B > 0.2$ ,  $c_p$  obtained by method (I) is moving away from the theoretical solution when  $B$  increases, and method (II) moving towards the theoretical solution.

It may also be observed that the difference in the location of the minimum  $c_p$  between method (I) and (II) decrease as  $Re$  increases. In all, it appears that method (I) gives the most consistent results when considering the minimum  $c_p$ .

For method (I) the general behavior of the  $c_p$ -curve when  $B$  increases is a less negative minimum value of  $c_{pb}$ , and an increasingly negative minimum  $c_p$ . This is also accompanied by a slight shift of this bottom towards higher  $Re$ . The base pressure,  $c_{pb}$ , increases slightly for almost all  $Re$  represented in this investigation, more on this in Section III-B.

### B. Base pressure

From Fig. 3 it is obvious that the behavior of  $c_{pb}$  is significantly different between (I) and (II), even more so than for  $C_L$  and  $C_D$  shown in Fig. 4.

For method (I)  $c_{pb}$  increases with  $Re$  and decreases with blockage; this is especially pronounced for *Setup B/C/D*. The decrease of  $c_{pb}$  with increasing blockage is approximately constant between *Setup A/B/C*. But, from *Setup C* to *Setup D* the decrease of  $c_{pb}$  is significantly larger, despite the fact that the increase in blockage is less than that between *Setup A* and *Setup B*. It is also worth noting that the variation of  $c_{pb}$  for *Setup A* is very small compared to that of *Setup B/C/D* at similar  $Re$ .

In *Setup A*, higher  $Re$  only leads to a minor increase of  $c_{pb}$ , and this increase is linear, not logarithmic in its shape as for *Setup B/C/D*.

*Setup D* reach values of  $Re$  above those found to be in the critical  $Re$ -range in Section III-D. In Fig. 3

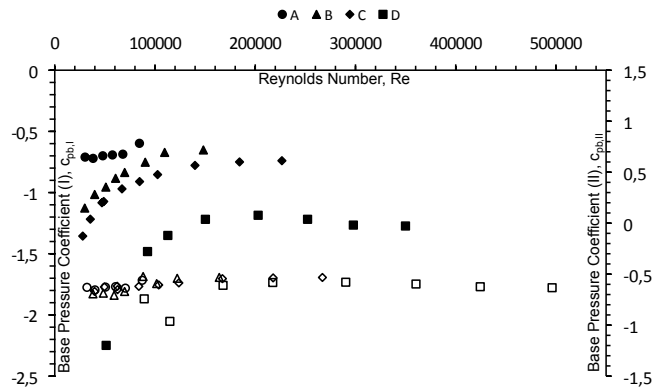


Fig. 3. Base pressure coefficient as a function of  $Re$  for all setups. Black markers are for method (I) and relates to the left vertical axis, grey markers are for method (II) and relates to the right vertical axis. Note that the vertical axes are only shifted vertically, thus keeping the shapes of the curves directly comparable.

a slight decrease is found for  $c_{pb}$  in both method (I) and (II) corresponding to the small increase in  $C_D$  for the highest  $Re$  measured in *Setup D*.

When applying method (II) to determine  $c_{pb}$  the results are strikingly different from those in (I). Now it appears that  $c_{pb}$  holds a nearly constant value of approximately  $-0.6$  over the whole  $Re$  range investigated.<sup>8</sup> Both dependance on blockage and  $Re$  appear almost nonexistent. The only variations within the  $Re$ -range used in these experiments are a slight increase for  $Re < 3 \cdot 10^5$  and a similar decrease for  $Re > 3 \cdot 10^5$ . But it has to be noted that this behavior can only be confirmed for *Setup D* which covers the whole range, and partly for *Setup B/C* which only covers  $Re < 1.5 \cdot 10^5$  and  $Re < 3 \cdot 10^5$ , respectively.

### C. Lift

The lift coefficient,  $C_L$ , over each cylinder is calculated by integrating the measured pressure distribution. Note that  $C_L$  is calculated assuming the pressure under the cylinder to be equal the measured static pressure. For the case of the half-buried pipeline this would mean that  $C_L$  is the upwards lift force created by the exposed part of the pipe, with a potential suction from the seabed counteracting it.

From potential flow theory it is expected that  $C_L \approx \frac{5}{3}$  for flow over a semi-circular floor-mounted cylinder.<sup>9</sup> In *Setup A*,  $C_L$  is found to be in the range  $1.36 - 1.77$ , with an average value of  $1.55$ . *Setup B/C/D* does not share this resemblance to the result from inviscid theory. Average values for  $C_L$

<sup>8</sup>The average  $c_{pb}$ , excluding *Setup D* for  $Re = 1.15 \cdot 10^5$  due to bad data, is:  $\bar{c}_{pb} = -0.6158$

<sup>9</sup> $C_L = \frac{1}{2} \int_0^\pi c_p \sin(\theta) \cdot d\theta$ ,  $c_p = 1 - 4 \cdot \sin^2(\theta)$

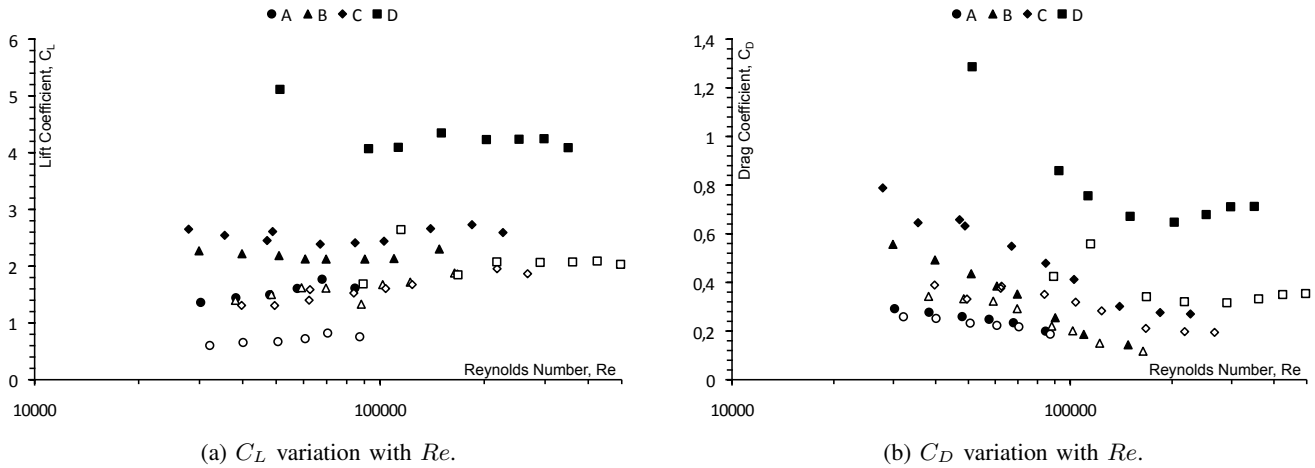


Fig. 4. Variation of  $C_L$  and  $C_D$  with the Reynolds number,  $Re$ . Filled markers are for method (I), outline markers are for method (II).

are 2.19, 2.55 and 4.30, with ranges of 2.12 – 2.30, 2.39 – 2.73 and 4.07 – 5.11, respectively.

The differences between method (I) and method (II) are pronounced. For method (I),  $C_L$  generally has a slight decrease at the lowest  $Re$  measured, followed by a slight increase, and a maximum close to the where minimum  $C_D$  is expected to be for the setup in question. Using method (II) to determine  $C_L$  gives substantially different results;  $C_L$  increases linearly from the lowest  $Re$  measured, until it reaches a maximum at approximately the same  $Re$  as the maximum in method (I). Neither the maximum values themselves, nor the decline after the maximums for *Setup A/C/D*, are drastically different. Although a slight decrease in the negative slopes may be observed. For *Setup B* the decline of  $C_L$  is not present for either method.

It also seems that there are a few bad measurements, even though these do not influence the conclusion, they will be reviewed briefly. For *Setup C* it appears that there are some problems with either series 2 or 3. This is not too problematic, as the general trend is unambiguous. The reason for this behavior is unclear, but as it exists both for method (I) and method (II), bad measurements for  $U_\infty$  or  $U_b$  are excluded. Consequently, it must be due to the measured pressure distribution around the cylinder.

For the first  $C_L$  measurement in *Setup D* it seems that the initial high  $C_L$  value for (I) is incorrect, and that there is no initial decrease in  $C_L$ . Judging from the  $c_p$  distribution, the reason for this inaccurate value is a bad measurement of  $U_\infty$ , resulting in similar inaccuracies for  $C_D$ , for method (I).

#### D. Drag

The drag coefficient,  $C_D$ , over each cylinder is calculated by integrating the measured pressure distribution. As the viscous drag becomes very small at higher  $Re$ , it is of little importance to the results and is thus omitted.

$C_D$  has a similar behavior for both (I) and (II), that is: a decreasingly negative slope, resulting in  $C_D$  leveling out. For *Setup D*, and presumably the other setups had  $Re$  been large enough,  $C_D$  starts increasing after remaining constant for a short  $Re$ -range. This behavior is directly comparable to the  $C_D$ -curve for circular cylinders in free flow in the critical  $Re$ -range. The critical  $Re$ -range for circular cylinders in free flow has been experimentally determined to be approximately  $1.4 \cdot 10^5 - 10^6$  [20]. Current findings also comply with those made by Wong (1981) [16] for flow over semi-circular floor-mounted cylinders; for a rough semi-circular cylinders  $C_D$  decreases rapidly before a slight increase just after  $Re \approx 10^5$ .  $C_D$  is reported to be nearly constant at higher  $Re$ . The critical Reynolds number,  $Re_{cr}$ , obtained in [16] is slightly higher than that obtained in the present investigation. This small deviation is discussed further in Section IV-E.

Although (I) is very similar to (II), the variations are larger, the initial decline is steeper and the slight incline after the bottom, for *Setup D*, is more pronounced for results obtained by method (I). Generally  $C_D$  increases with blockage and aspect ratio for both methods, shifting the curves to higher  $C_D$ . This shift of the  $C_D$ -curves grows with increasing  $B$ . The growth relative to the last increase of  $B$  is larger for (I) than for (II). All the curves are also shifted to higher  $Re$  due to the flow acceleration

above the cylinder in method (II), with the low blockage setups being shifted less than the high blockage setups.

Similar to  $C_L$ , the effects of the bad measurements are also found here. The deviations that exist are apparent, but not of any significance to the final results as general trends are still discernible.

### E. Velocity profiles

Velocity profiles were determined for *Setup A/C/D* at given  $Re$ , corresponding with those given in Table II. Measurements were also performed for similar  $U_\infty$ , *without* the cylinders installed. In order to compare velocity profiles obtained with and without blockage, the empty tunnel velocity profiles are shifted horizontally, such that a given  $U_\infty$  for the empty tunnel is *identical* to that of the setup and  $Re$  it is compared to. This is done by multiplying the results for the empty wind tunnel with the ratio between  $U_\infty$  with the cylinders and  $U_\infty$  without the cylinders installed.

*Setup B* was left out as the goal of these measurements was to map the development of the flow between the top of the cylinder and the roof of the wind tunnel, and not to acquire an accurate description of the flow above the cylinders.

Looking at the acceleration of the flow immediately above the cylinders, a discrepancy between the measurements and the expected results was found. For all cases a very sharp increase of the flow velocity should be located immediately above the cylinder. According to potential flow theory the flow velocity on top of the cylinder should be  $\approx 2U_\infty$ . This was obviously not the case for neither of the setups. The reason for this is probably the distance between where the static and the stagnation pressures are measured, the latter being located about 3 cm downstream of the first. It is believed that this occurs when the static pressure probe is located close to, in the boundary between the recirculation zone and the free flow, or in the separated flow behind the cylinders. For such occurrences the static pressure probe would not measure solely the static pressure, but the static pressure with some additional pressure. This will give a larger reading of the static pressure, which in turn leads to a lower reading for the flow velocity. Also, if the flow is not completely parallel to the pitot probe, i.e. the flow is not horizontal but the pitot is, a similar effect will be observed.

It has been shown, by comparing pitot-tube measurements with hot-wire measurements, that

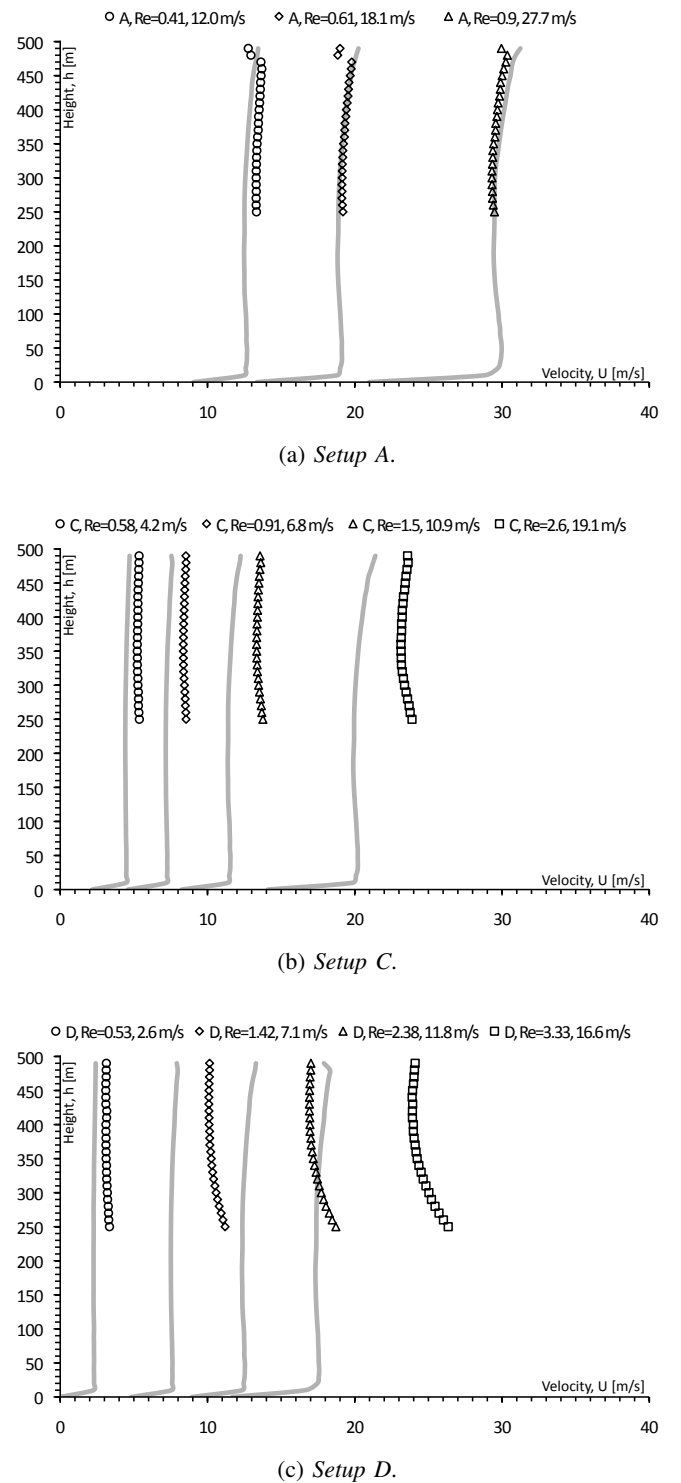


Fig. 5. Velocity profiles for *Setup A/C/D*. Markers indicate the velocity distribution measured with the cylinders installed. Grey lines represent the velocity distributions without the cylinders installed. The distributions for the empty wind tunnel were measured at wind speeds,  $U_\infty$ , comparable to those with the cylinders installed. The empty tunnel measurements were then shifted horizontally to correct for deviations in  $U_\infty$ . This was done by multiplying the results for the empty wind tunnel with the ratio between  $U_\infty$  with the cylinders and  $U_\infty$  without the cylinders installed.

these effects disappear only a small distance over the cylinders, after which the results for the two measurement methods conform [24]. The use of these velocity profiles in the current investigation

does not rely on an accurate description of the speed-up immediately above the cylinder, where the measurements have been proven to be inaccurate, but rather the knowledge of the overall behavior of the bulk flow over each cylinder. Therefore, the errors encountered with the pitot-measurements are not of any significance, as they will not influence the perceived behavior of the velocity profile in the area that is currently interesting. The measurements considered to be erroneous on the basis of the discussion above are *not* shown in Fig. 5. Note that a generous safety margin was used when removing incorrect measurements.

For *Setup A* the influence of the blockage is barely noticeable; the speed up over the cylinder is evident, but the flow velocity normalizes within 250 mm of the floor, and there is no overall increase of the bulk flow velocity above the cylinder.

*Setup C* has a blockage ratio of 0.198, and a larger influence on the overall velocity profiles is expected. Considering Fig. 6 for the lowest  $Re$ , corresponding to  $U_\infty = 4.21$  m/s, the influence is comparable to what is considered random variation in *Setup A*. However, as  $Re$  increases it is evident that the presence of the blockage accelerates the bulk flow velocity above the cylinder significantly.

*Setup D* exhibits a behavior nominally similar to that of *Setup C*, but the acceleration of the bulk flow velocity above the cylinder is considerably larger.

The percentage differences between the empty wind tunnel and the cases of the installed cylinders, for a given blockage, are presented in Fig. 6. These appear fairly constant, with average values of 1%, 15% and 36% for *Setup A/C/D*, respectively. Some variation is found in this percentage value within each setup at different  $Re$ . In *Setup C/D* these fluctuations appear random and are discarded as measurement errors, or as a result of transient effects in the flow. As for *Setup A*, there appears to be a slight negative slope without any evident explanation. The most probable cause again appear to be natural variation of the measurements.

### F. Vortex shedding

Spectral analysis of the time-series, obtained by use of a hot-wire anemometer in different parts of the wake, do not show any dominant frequencies for any of the cylinders or  $Re$  investigated in these experiments.

## IV. ANALYSIS

### A. Unit Reynolds number effects

It is important to note that unit Reynolds number effects may exist. These are the dependance of

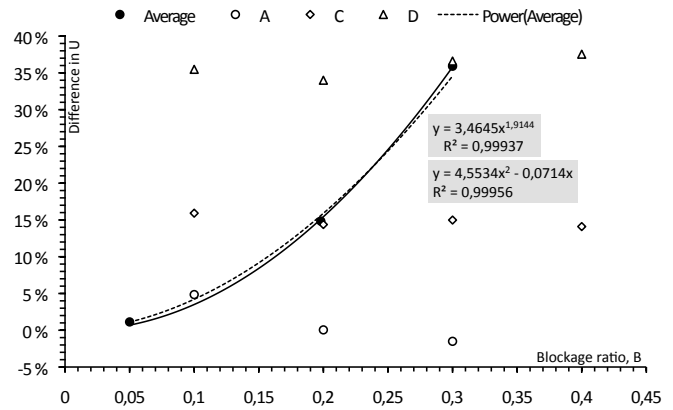


Fig. 6. An overview of the velocity changes for the different setups. Black markers indicate the average percentage velocity increase for a given blockage. The solid black line is a best fit curve for the three aforementioned black markers. Note that markers with white fill does not relate to the horizontal value axis, only the vertical.

the pressure distribution curve on other variables than the Reynolds number. Effects include, but are not necessarily limited to: the aspect ratio  $L/D$ , the relative surface roughness  $\epsilon/D$ , the turbulence scale parameter  $\lambda/D$  and the turbulence intensity  $u'/U$  [25].

The turbulence intensity is relatively constant for the  $U_\infty$  used in these experiments [17]. It is also assumed that the difference in the turbulence scale parameter are negligible. Also the surface roughness is considered to be constant for all the cylinders used. Thus, of the potential effects identified, the aspect ratio of the cylinders is left as the most probable cause of unit Reynolds number effects.

For circular cylinders it has been shown that both increase in aspect ratio and increase in blockage lead to a decrease of  $C_D$  and a decrease of  $c_{pb}$  [26], this is discussed further in Section IV-F.

In this analysis the effects observed have been attributed to either the change in  $Re$ , or a combination of increase in blockage,  $B$ , and decrease of aspect ratio,  $L/D$ .

### B. Pressure distribution

The solution for  $c_p$  from potential flow theory describes the *ideal flow*, and does not account for neither separation from the cylinder, nor blockage or wall effects. This explains the obvious deviations between this potential theory and the results from the present investigation shown in Fig. 2.

The initial  $c_p$ -value is 1 for the theoretical solution, but takes on a value of approximately 0.5 for all the measured results. This is similar to previous results for flow over a semi-circular cylinder mounted to a plane surface at similar  $Re$  [14][15][16][27].



The measured values of  $c_p$  for the lowest  $\theta$ -angles do also exhibit a slight increase. It is believed that the reason for this initial increase not being present in the results for *Setup A* is poor resolution of the pressure taps. Its occurrence in *Setup B/C/D* is thus *not* considered a result of blockage. Consequently, the increase in *Setup B/C/D* is believed to be solely due to the boundary layer created by the floor. A similar result was obtained in [16].

What is interesting to note is that for both method (I) and method (II), the negative slope for  $20^\circ \leq \theta_a \leq 70^\circ$  increases with increasing blockage. This will give a more adverse pressure gradient, which in turn is believed to bring with it a lower  $Re_{cr}$ . A similar effect was observed in [28] for closely spaced cylinders.

Method (II) is believed to somewhat counteract the effects of solid blockage. It appear that the desired effect is achieved to a certain extent. This will be discussed further throughout this the analysis.

### C. Base pressure

From Fig. 3 it appears that using method (II) renders  $c_{pb}$  less dependent of blockage, and all measurements for  $c_{pb}$  collect around a common value of approximately 0.6. The only dependance that may be found is a slight overall increase of  $c_{pb}$  with increasing  $Re$ . Judging by *Setup D* alone, it appears that this increase continues until  $Re$  is between  $2 \cdot 10^5$  and  $3 \cdot 10^5$ . Following this,  $c_{pb}$  starts decreasing in a fashion similar to that for method (I). It is natural to assume that the cause of this decrease in (II) is due to the same effects as in (I), inferring that the reason for this change is close to independent of the acceleration of the flow, and rather related to either a shift in the separation point, or a change in the wake structure. A look at the  $C_D$ -curves in Fig. 4b supports the former by exhibiting a minimum around  $2 \cdot 10^5 - 3 \cdot 10^5$  corresponding with the maximum of the  $c_{pb}$ -curve. This minimum of the  $C_D$ -curve is then followed by a slight increase that is in agreement with the small decrease in  $c_{pb}$ .

It is very interesting to observe that the behavior of the  $c_{pb}$ -curve for *Setup A* in Fig. 3 is nearly the same for method (I) and (II). Only a negligible decrease of the positive slope may be observed. Base pressure values for all setups in method (II) appear to be located around the same value and exhibiting the same general trend with change in  $Re$ . The more consistent value of  $c_{pb}$  is also very close to that from some prior investigations [15][16] of low blockage flow. Thus it seems that using  $U_b$  as

the reference velocity offers a good correction for blockage-effects on  $c_{pb}$ , at least up to  $Re \approx 1.5 \cdot 10^5$ .

It is also worth noting that the values of  $c_{pb}$ , in (II), are similar for those found for a circular cylinder in cross-flow, laid on a plane surface with comparable  $Re$  [1]. For method (I) the similarity decreases with an increase of blockage, and for low  $Re$  the deviation is large for all blockages.

### D. Lift

From inviscid theory it is expected that  $C_L \approx \frac{5}{3} \cdot 10$ .<sup>10</sup> In accordance to this, the measured  $C_L$  does not vary drastically with  $Re$  for neither method (I) nor method (II). It is clear that the lift of a given cylinder is almost independent of  $Re$  for the range covered in the present investigation.

The  $C_L$  values found for *Setup A* are close to those found by potential flow theory. The small deviations that exist are most likely due to the fact that this theory neglects turbulent separation, separation bubbles, blockage effects and wall effects, all of which contribute to change the flow over the cylinder. Also note that the resolution of pressure taps on the cylinder in *Setup A* is relatively poor due to its small size, and that this may contribute to the difference.

Toy and Tahouri (1988) [15] found that  $C_L$  was 0.63 for  $Re \approx 1.32 \cdot 10^5$ . This value is about half that of the lowest  $C_L$  found in the current investigation with  $U_\infty$  as the reference velocity. It is not believed that this difference is due to blockage. Unit Reynolds number effects resulting from differing properties of the experiments, such as incoming boundary layer, surface roughness and pressure tap resolution are the most likely causes. Although, there is not enough information available in [15] to be certain.

For *Setup B/C*, method (I), a similarity between the two setups with regards to the variation of  $C_L$  may be observed. Both setups have a slight decrease of  $C_L$  from  $Re \approx 3 \cdot 10^4$  that flattens out around  $Re \approx 6 \cdot 10^4$ , and subsequently starts increasing from  $Re \approx 10^5$ . The reason for this behavior is unclear. It was initially believed that it was due to the occurrence of a laminar separation bubble in the flow over the semi-circular cylinder. However, this explanation is somewhat problematic, as the behavior of *Setup B/C* for (II) exhibits a nearly opposite trend, with a slight but steady *increase* of  $C_L$ . A similar opposite relationship between  $C_L$ -curves is also present in *Setup D*, but not in *Setup A*.

<sup>10</sup> $C_L = \frac{1}{2} \int_0^\pi c_p \sin(\theta) \cdot d\theta$ ,  $c_p = 1 - 4 \cdot \sin(\theta)$

The latter observation is interesting, indicating that blockage is at least a contributing, if not the main cause, of the observed behavior in *Setup B/C/D*. Thus it seems that once more the dependance on blockage is expressed better by method (I), and appear to be somewhat accounted for by using method (II).

As documented in several studies on circular cylinders [22][29][30], the separation point varies between  $70^\circ$  and a maximum of  $140^\circ$  from the leading edge. The location of the separation point also depends on the type of separation. Laminar separation is found to occur at  $70^\circ - 80^\circ$ . Moving into the critical  $Re$ -range, a laminar separation followed by reattachment and a turbulent final separation has been found around  $110^\circ - 140^\circ$ . This state may exist up to  $Re \approx 1.5 \cdot 10^6$  where, for smooth cylinders, the flow enters the supercritical range. Now the separation point moves upstream again to about  $110^\circ$  [31]. Later works have described these experimentally observed effects in more detail [32].

Results from method (I) suggests that a process similar to that of the separation bubble on circular cylinders in free flow also occurs in the current investigation. In Fig. 4b,  $C_D$  for *Setup B/C* method (I) decreases for the whole range of  $Re$  covered. This would imply, using the flow regimes described above, that the separation point moves downstream for  $Re > 10^5$ . It is likely that this is due to a laminar separation bubble which, for circular cylinders in free flow, occurs in the declining part of the  $C_D$ - $Re$ -curve. This region is commonly referred to as the critical  $Re$ -range.

Existence of separation bubbles in the current experiments is also supported by the behavior of the  $C_D$ - $Re$ -curve for *Setup D* in Fig. 4b, whose shape clearly resembles that of flow around two-dimensional circular cylinders. In addition, evidence of separation bubbles is found in some of the  $c_p$ - $\theta$ -curves in Fig. 2.

A separation bubble is indicated by a discontinuity in the  $c_p$ -curve [33], and may exist exclusively on one, both, or alternating sides of a cylinder [34]. Separation bubbles are also found to disappear when critical  $Re$  is achieved [31], although it has to be noted that this is not always the case [35].

Observing the  $c_p$ -curves for *Setup B/C/D* in Fig. 2d/2c, there are indications of separation bubbles for series 1-6, 1-5 and 1-3, respectively. Using method (I) this correspond to:  $Re = 0.3 \cdot 10^5 - 0.70 \cdot 0.10^5$ ,  $Re = 0.28 \cdot 10^5 - 0.67 \cdot 0.10^5$  and  $Re = 0.51 \cdot 10^5 - 1.13 \cdot 10^5$ . These  $Re$ -ranges coincide with the ranges where  $C_D$  decreases. When

$Re$  increases, the separation bubble will decrease in both length and height [36]. Due to this change in the shape of the separation bubble, the displacement added to the flow around the cylinder is also decreased<sup>11</sup> [37], resulting in a decrease of  $C_L$ . The occurrence of separation bubbles decreases with  $Re$ , purely turbulent separation starts to take over, and the  $C_L$ -curve levels out. This happens for  $Re$  between  $0.61 \cdot 10^5 - 1.1 \cdot 10^5$  for *Setup B* and  $0.67 \cdot 10^5 - 1.03 \cdot 10^5$  for *Setup C*, corresponding to measurements series 4-7 and 5-7, respectively.

It is difficult to determine whether separation bubbles are suppressed or exaggerated by the increase in  $B$ . From Fig. 4 it appears that the initial decline of  $C_D$  is steeper for higher  $B$ . This could indicate a more rapid succession through the regime where bubbles are present. Such an effect has been shown for closely spaced circular cylinders in cross-flow [28].

In *Setup A* the resolution is too poor to conclude whether or not bubbles are present.

The increase of  $C_L$  starting at  $Re \approx 1.03 \cdot 10^5$  for *Setup C*, leads to what appears to be maximum for both (I) and (II). It also seems that the same maximum, using its occurrence in relation to minimum of the  $C_D$ -curves as a reference, would be present in *Setup B* if higher  $Re$  had been achieved. Furthermore the maximum is weakly indicated in *Setup D* where it is expected to be in relation to the considerations for *Setup B/C*.

As for *Setup A*, there exists a maximum for  $Re \approx 0.68 \cdot 10^5$ , but it does not appear that it relates to the  $C_D$ -curve in a similar manner to what was found for *Setup B/C/D*. The reason for this maximum is unclear, and cannot be explained by the mechanism mentioned above. From Fig. 3 it is also evident that  $c_{pb}$  is also more or less constant for the area in question, eliminating a change in  $C_b$  as the reason for the observed behavior.

### E. Drag

As inviscid theory predicts zero drag for all shapes that are symmetrical along a plane normal to the flow direction, it may not be used to obtain an estimate for  $C_D$  for a semi-circular cylinder.

Toy and Tahouri (1988) [15] found  $C_D = 0.26$  for  $Re \approx 1.32 \cdot 10^5$ . This value is close to  $C_D$  found in *Setup A* for method (I) at the lowest  $Re$  measured. The difference grows with increasing blockage, more so for method (I) than for method (II), indicating that the latter method somewhat counteracts the effect of solid blockage. The slightly

<sup>11</sup>Separation bubbles do not influence momentum thickness.

elevated  $C_D$  in the present investigation, for *Setup A* and  $Re$  close to that in [15], may be due to higher surface roughness in the current experiments or differences in  $I_u$  which both lower the critical  $Re$  for circular cylinders [21][22][23], as mentioned in Section III-D.

Current findings also comply with those made by Wong (1981) [16] for flow over semi-circular floor-mounted cylinders; for a rough semi-circular cylinder  $C_D$  decreases rapidly before a slight increase just after  $Re \approx 10^5$ .  $C_D$  is reported to be nearly constant at higher  $Re$ . The critical Reynolds number,  $Re_{cr}$ , obtained in [16] is slightly higher than that obtained in the present investigation. This small deviation is most likely due to lower roughness on the cylinder surface, and possibly higher incoming  $I_u$ , in the current experiments. A change in any of these two will lead to a lower critical of  $Re$  for circular cylinders [21][22][23]. It is believed that a change in these parameters will have the same effect for the current case.

Similar to the behavior of  $C_L$ , the dependance on blockage seems to be expressed better by method (I), and appears to be somewhat counteracted by using method (II).

The results obtained in the present investigation exhibit an overall behavior similar to that of circular cylinders in free flow for critical  $Re$ . For all the setups, and both method (I) and method (II), a steady decrease is found. Observing the drag curves for *Setup C/D*, and partly *Setup B*, in Fig. 4b, it may be observed that this decrease flattens as  $Re$  increases. For circular cylinders in free flow, the decrease of  $C_D$  in the critical  $Re$  regime is mainly contributed to a turbulent destabilization of the flow, the occurrence of one- or two-sided laminar separation bubbles that shift the final separation backwards, and an increase in the Strouhal number,  $St$  [20][33]. For the case of the current experiments, the latter is not an influence as no vortex shedding occurs, see Section IV-H. As for the laminar separation bubbles, it is believed that they play the main part in the steady decrease of  $C_D$ . As substantiated in Section IV-D, separation bubbles appear to occur for *Setup B* series 1 – 6, *Setup C* series 1 – 5 and *Setup D* series 1 – 2, in addition to a weak indication for series 3 in the latter setup.<sup>12</sup> These bubbles are presumably the reason for the initial decrease, followed by a stabilization and, for *Setup D*, a slight increase moving to higher  $Re$ .

<sup>12</sup>Using method (I) this corresponds to  $Re = 0.3 \cdot 10^5 - 0.70 \cdot 10^5$ ,  $Re = 0.28 \cdot 10^5 - 0.67 \cdot 10^5$  and  $Re = 0.51 \cdot 10^5 - 1.13 \cdot 10^5$ , respectively.

Having accounted for the main trends of  $C_D$ , focus is directed towards identifying the effects of the variation of blockage and aspect ratio on  $C_D$ . For method (II),  $C_D$  exhibits less spread, variation for a given setup are less pronounced, and all the values are shifted somewhat towards higher  $Re$ . The shift is due to the increase in the reference flow velocity when using method (II).

As the blockage  $B$  increases, the growth of  $C_D$  between setups becomes larger. Although the blockage increase from *Setup A* to *Setup C* is larger than that between *Setup C* and *Setup D*, the overall increase of  $C_D$  between the latter configurations is significantly larger. Thus it seems that the growth does not relate linearly to  $B$ , more on this in Section IV-F.

By assuming that method (II) to some extent counteracts the blockage, the decreased distance separating the  $C_D$ -curves between method (I) and (II) gives an indication to the extent of the effect of solid blockage. This gap appear to grow with increasing  $B$ . It should be noted, from *Setup A*, that a very small gap between (I) and (II) does exist, but it is small enough to assume that *Setup A* is independent of blockage. For method (II) the spread of  $C_D$  decreases as  $Re$  increases, this is also true for method (I), but not to the same extent. Since the solid blockage seems largely accounted for by use of  $U_b$  as the reference velocity, the difference found for method (II) is suspected to be mainly a result of wake blockage.

For *Setup A/B/C* no significant variation in the distance between the  $C_D$ -curves may be observed for the lowest  $Re$ . In addition, the differences between (I) and (II) seem to decrease as  $Re$  increases. It is believed that the reason for this is complex, but one part of the puzzle is thought to be the movement of the point for final separation from the cylinder, as described in Section IV-D. When separation occurs at low  $\theta$ , the initial wake region is larger than if separation occurs further downstream. Thus the wake from early separation requires more space to develop as normal for a given length downstream, than that from a later separation. When  $Re$  increases and the point of separation is moved backwards, the initial size of the wake is reduced and the restriction on normal development is smaller. This is also somewhat supported by the behavior of  $c_{pb}$  for method (I), Fig. 3; for low  $Re$   $c_{pb}$  has a significantly lower value than for high  $Re$ . Assuming similar flow mechanism to circular cylinders would mean that the wake is larger for low  $Re$  [25]. As  $Re$  increases, the change of  $c_{pb}$  suggest that the wake, and point of separation, remains roughly

constant. This could explain why the the difference between the  $C_D$  curves is smaller, and more stable, at higher  $Re$ . By applying method (II), the variation of  $c_{pb}$  is significantly reduced. There is however a trend suggested through a slight increase with a maximum around  $2 \cdot 10^5 - 3 \cdot 10^5$ , which correlates well with the explanation presented above.

#### F. Blockage and aspect ratio

Reduction in aspect ratio and an increase in blockage have the same effects on  $C_D$  and  $c_{pb}$  [26]. Since the blockage ratio in the current experiments increase with decreasing aspect ratio, it is hard to separate their influence on the results. However, the goal of these experiments is to map the effects that may be contributed to a given experimental setup, rather than the real case modeled. Thus, a consideration of the effects of change in blockage and aspect ratio combined will be performed. Such a combined variation is the case for many investigations, as the models often span the whole width of the test section to give nominally 2D flow.

Looking at Fig. 7 it may be noted that the values of  $c_{pb}$  found in the current experiments are somewhat larger than those found by West and Apelt (1982) [26] during their experiments with polished brass tubes. It has been shown in earlier investigations that as a cylinder in cross-flow comes close to a plane surface parallel to the flow, e.g. the wind tunnel floor,  $c_{pb}$  decreases [1][38]. Bearman and Zdravkovich (1978) [1] contributed this effect to weakening of the shed vortices, possibly in combination with a change in their position. In addition they showed that the variation of  $c_{pb}$  with  $Re$  has the same shape, independent of the gap between the cylinder and the wall. It is believed that these relationships are transferrable to the half-buried cylinders in present investigation. Thus, the variation of  $c_{pb}$  with blockage and aspect ratio for a circular cylinder will have a comparable shape to that of the semi-circular floor-mounted cylinders in the present investigation, but not necessarily the same values.

From Fig. 7a it is clear that the shape of the  $c_{pb}$ - $B$ -curve found in [26] for  $Re = 0.45 \cdot 10^5$  and  $L/D = 6$  is in good agreement with those obtained in the present experiments when considering the shape only. What is interesting to see is that for the higher blockages, measurements indicate an accelerated decrease in  $c_{pb}$ . This decrease is not in compliance with the linear nature of the measurements by West and Apelt (1982) [26].

For the variation with aspect ratio, a trend similar to that of  $c_{pb}$ - $L/D$ -curve, for  $Re = 0.33 \cdot 10^5$  and

$B = 0.06$  from [26], is found. The main difference is the decrease towards the end appears drastically increased. Interestingly, the reduction of  $c_{pb}$  is larger for lower  $Re$ , suggesting that blockage and aspect ratio effects on  $c_{pb}$  are larger for lower  $Re$ . It appears that as the aspect ratio decreases, the effect of a unit change of the aspect ratio will increase.

As shown in [26] for a circular cylinder, the variation of  $L/D$  has only a slight and linear influence on  $c_{pb}$  until  $L/D \approx 10$ . For  $L/D < 10$  the influence strengthens and the slope becomes increasingly negative. A similar behavior may be found for all  $Re$  in Fig. 7a/7b. Hence, it is believed that the main cause of the steep decrease in  $c_{pb}$  is due to the superimposition of the linear decrease in  $c_{pb}$ , resulting from an increase in  $B$ , and the linear, then accelerating for  $L/D < 10$ , decrease of  $c_{pb}$  resulting from the decrease of  $L/D$ .

#### G. Velocity profiles

The effect of the blockage on the velocity profiles obtained in the flow between the cylinders and the roof is fairly close to what is expected; for low blockages no effect on the bulk flow velocity may be observed, but for higher blockages the influence of the cylinders on the flow is significant. From Fig. 6 it may be deduced that, for a given blockage, the bulk flow velocity above the cylinders does not increase linearly with  $U_\infty$  for a given  $B$ , but rather proportional to a speed up ratio,  $K$ .

Two trend lines have been inserted into Fig. 6, one polynomial fit and one power fit. Both indicate that  $K \propto B^2$ .<sup>13</sup> This suggests that the governing factor for the variation of the speed-up over the blockage is the volume displaced, which indicate that

By observing Fig. 5 for all  $U_\infty$  and  $B$ , it is found that the flow close to the roof, where  $U_b$  is measured, mainly show a horizontal translation of the velocity profile. Thus, it may be concluded that  $U_b$  used in method (II) gives a good representation of the bulk flow velocity in the constricted part of the flow.

#### H. Vortex shedding

No dominant frequencies were observed. It is thus concluded that no regular vortex shedding occurs for the case of the half-buried cylinder. As vortex shedding predominately is a result of interaction between the flow on either side of the cylinder [39], it comes as no surprise that traditional vortex shedding is not found. The results obtained in the present experiments are consistent with previous

<sup>13</sup> $V_{\text{half cylinder}} = \frac{\pi}{4} h^2 l$  and  $h = B \cdot H$ .

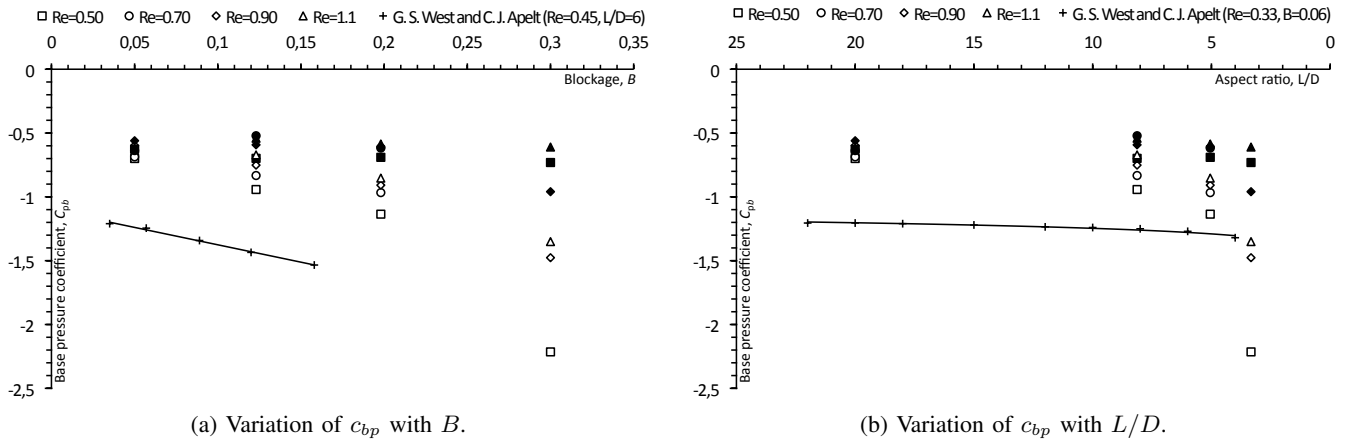


Fig. 7. Variation of the base pressure coefficient,  $c_{pb}$ , with blockage,  $B$ , and aspect ratio,  $L/D$ . Note that the Reynolds number is given as  $Re \cdot 10^{-5}$ .

results obtained for circular cylinder laid on a plane surface [1][40].

## V. CONCLUSION

It was observed that for  $B = 0.05$ , no effects of blockage were present, regardless of  $Re$ .

The acceleration of the flow between the top of the cylinders and the roof appear to be relatively constant for a given blockage. The speed-up ratio,  $K$ , was found to be proportional to  $B^2$ .

Except for the general increase in flow velocity, the flow close to the roof is not directly influenced by the cylinder. In terms of the velocity profiles plots, the flow is merely shifted horizontally towards higher  $U$ .

Using  $U_b$  as the reference velocity is, with some limitations, an effective method for dampening the influence of *solid blockage* in the final result. It also seems that the influence of aspect ratio to some extent is accounted for by this definition.

The base pressure,  $c_{pb}$ , complies significantly better with results from other investigations without blockage, for all  $Re$  used, when it is calculated by method (II). The results also indicate that method (II), at the lower  $Re$  investigated, partly accounts for the growth restrictions imposed on the wake by the wind tunnel. It was not possible to determine the exact mechanisms behind this in the current investigation. The belief is that this is connected to the recirculation zone behind the cylinder, which is larger for low  $Re$  due to earlier separation, exercising a direct influence on the flow over the cylinder by increased displacement.

For these experiments, variation of the blockage and the aspect ratio were not kept separate. This is the case for most investigations not solely focusing on these effects. Since the variation of one of these

led to a variation in the other, both with the same effect on the flow, only a conjoint analysis could be performed. The effect of these appear to be dominated by the  $B$  for  $L/D > 10$ , corresponding to  $D = 0.1\text{m}$ . For  $L/D < 10$ ,  $B > 0.10$ , the influence on  $c_{pb}$  is drastically increased. It is believed that the aspect ratio is the main cause for the increased influence when  $L/D < 10$ . Consequently it is suggested that this is attributable to the flow becoming three-dimensional as a result of influence from the wind tunnel side walls. On this basis it would not be recommendable to operate with  $L/D < 10$  when the blockage spans the whole width of the wind tunnel, as the decline of  $c_{pb}$  accelerates violently below this limit.

It was not possible to determine with certainty whether separation bubbles are suppressed or exaggerated by the increase in  $B$ . Based on the flow regimes defined for circular cylinders, it appears that separation bubbles occur at the same  $Re$ -ranges relative to the  $C_D$ -curve. However, from Fig. 4 it seems that the initial decline of  $C_D$  is steeper for higher  $B$ . This may indicate a more rapid succession through the regime where bubbles are present.

As for circular cylinders laid on plane surfaces, no regular vortex shedding occurs for the  $Re$  used in the current investigation.

## ACKNOWLEDGMENTS

I would like to take this opportunity to thank my supervisor, Professor Lars R. Sætran for his support, help and guidance. I would also like to express my gratitude to the workshop supervisor at the "Fluids Engineering Lab", Arnt Egil Kolstad, for all his help in preparing the experiments.

APPENDIX A  
LIST OF SYMBOLS

Table III offers an overview of the symbols used in this article and their definitions, where applicable.

TABLE III  
COMPLETE LIST OF SYMBOLS USED AND THEIR DEFINITIONS,  
WHERE APPLICABLE.

Symbol	Unit	Description	
$A$	$m^2$	Projected area normal to flow	-
$U_\infty$	$\frac{m}{s}$	Flow velocity	-
$U_t$	$\frac{m}{s}$	$U$ , top of the cylinder	-
$U_b$	$\frac{m}{s}$	Bulk flow velocity	-
$F_D$	$\frac{kg \cdot m}{s^2}$	Lift	-
$F_L$	$\frac{kg \cdot m}{s^2}$	Drag	-
$D$	m	Diameter	-
$l$	m	Cylinder length	-
$h$	m	Cylinder height	-
$H$	m	Wind tunnel height	-
$f_v$	$\frac{1}{s}$	Vortex shedding frequency	-
$\theta_a$	$^\circ$	Degrees from upstream edge	-
$\theta$	rad	Radians from upstream edge	-
$\nu$	$\frac{m^2}{s}$	Kinematic viscosity	-
$B$	-	Blockage ratio	$\frac{h}{H}$
$K$	-	Speed-up ratio	$\frac{U_\infty}{U_b}$
$I_u$	-	Turbulence intensity	$\frac{\sqrt{u'^2}}{u}$
$c_{p,(I)}$	-	Pressure coefficient method (I)	$\frac{p-p_\infty}{\frac{1}{2}\rho U_\infty^2}$
$c_{p,(II)}$	-	Pressure coefficient method (II)	$\frac{p-p_\infty}{\frac{1}{2}\rho U_b^2}$
$c_{pb,(I)}$	-	Base pressure coefficient method (I)	$\frac{p_b-p_\infty}{\frac{1}{2}\rho U_\infty^2}$
$c_{pb,(II)}$	-	Base pressure coefficient method (II)	$\frac{p_b-p_\infty}{\frac{1}{2}\rho U_b^2}$
$C_{D,(I)}$	-	Drag coefficient method (I)	$\frac{F_D}{\frac{1}{2}\rho U_\infty^2 A}$
$C_{D,(II)}$	-	Drag coefficient method (II)	$\frac{1}{2} \int c_{p,(I)} \cos(\theta) d\theta$ $\frac{F_D}{\frac{1}{2}\rho U_b^2 A}$
$C_{L,(I)}$	-	Lift coefficient method (I)	$\frac{1}{2} \int c_{p,(II)} \cos(\theta) d\theta$ $\frac{F_L}{\frac{1}{2}\rho U_\infty^2 A}$
$C_{L,(II)}$	-	Lift coefficient method (II)	$\frac{1}{2} \int c_{p,(I)} \sin(\theta) d\theta$ $\frac{F_L}{\frac{1}{2}\rho U_b^2 A}$
$Re_{(I)}$	-	Reynolds number method (I)	$\frac{U_\infty D}{\nu}$
$Re_{(II)}$	-	Reynolds number method (II)	$\frac{U_b D}{\nu}$
$Re_{cr}$	-	Critical Reynolds number	$\frac{U_{cr} D}{\nu}$
$St$	-	Strouhal number	$\frac{f_v D}{U}$

REFERENCES

- [1] P. W. Bearman and M. M. Zdravkovich, "Flow around a circular cylinder near a plane boundary," *Journal of Fluid Mechanics*, vol. 89, no. 01, pp. 33–47, 1978.
- [2] M. Zdravkovich, "Forces on a circular cylinder near a plane wall," *Applied Ocean Research*, vol. 7, no. 4, pp. 197–201, 1985.
- [3] T. C. Sumer, B. M., T. Sichmann, and J. Fredsøe, "Onset of scour below pipelines and self-burial," *Coastal engineering*, vol. 42, no. 4, pp. 313–335, 2001.
- [4] F. Hatipoglu and I. Avci, "Flow around a partly buried cylinder in a steady current," *Ocean Engineering*, vol. 30, no. 2, pp. 239–249, 2003.
- [5] S. Cokgor and I. Avci, "Hydrodynamic forces on partly buried tandem, twin pipelines in current," *Ocean Engineering*, vol. 28, no. 10, pp. 1349–1360, 2001.
- [6] S. Cokgor, "Hydrodynamic forces on a partly buried cylinder exposed to combined waves and current," *Ocean Engineering*, vol. 29, no. 7, pp. 753–768, 2002.
- [7] V. Jacobsen, M. Bryndum, and C. Bonde, "Fluid loads on pipelines: sheltered or sliding," in *Offshore Technology Conference*, 1989.
- [8] V. Jacobsen, "Forces on sheltered pipelines," in *Offshore Technology Conference*, 1988.
- [9] N. Ismail, N. Wallace, and R. Nielsen, "Wave forces on partially buried submarine pipelines," in *Offshore Technology Conference*, 1986.
- [10] A. Fyfe, D. Myrhaug, and K. Reed, "Hydrodynamic forces on seabed pipelines: Large-scale laboratory experiments," in *Offshore Technology Conference*, 1987.
- [11] M. Parker and J. Herbich, "Drag and inertia coefficients for partially-buried offshore pipelines," in *Offshore Technology Conference*, 1978.
- [12] J. D. Guldsten and G. Zarraonandia, "Influence on wind shear and turbulence in flow over obstacles," Master's thesis, Norwegian University of Science and Technology, 2010.
- [13] M. D. Griffith, M. C. Thompson, T. Leweke, K. Hourigan, and W. P. Anderson, "Wake behaviour and instability of flow through a partially blocked channel," *Journal of Fluid Mechanics*, vol. 582, pp. 319–340, 2007.
- [14] T. Ogawa, M. Nakayama, S. Murayama, and Y. Sasaki, "Characteristics of wind pressures on basic structures with curved surfaces and their response in turbulent flow," *Journal of Wind Engineering and Industrial Aerodynamics*, vol. 38, no. 2-3, pp. 427–438, 1991.
- [15] N. Toy and B. Tahouri, "Pressure distributions on semi-cylindrical structures of different geometrical cross-sections," *Journal of Wind Engineering and Industrial Aerodynamics*, vol. 29, no. 1-3, pp. 263–272, 1988.
- [16] C. Wong, "The structural behaviour of braced barrel vaults with particular reference to wind effects," *Theses from the University of Surrey*, p. 111, 1981.
- [17] L. R. Sætran, "The wind tunnel at 'Institutt for mekanikk', NTH," Norges Tekniske Høgskole, Universitetet i Trondheim, Tech. Rep. 83:3, 1983.
- [18] C. Grant, R. Dyer, and I. Leggett, "Development of a new metocean design basis for the nw shelf of europe," in *Offshore Technology Conference*, 1995.
- [19] A. Palmer and R. King, *Subsea pipeline engineering*. PennWell Books, 2004.
- [20] H. N. Niemann, H. J., "A review of recent experiments on the flow past circular cylinders," *Journal of Wind Engineering and Industrial Aerodynamics*, vol. 33, no. 1-2, pp. 197–209, 1990.
- [21] E. Szechenyi, "Supercritical reynolds number simulation for two-dimensional flow over circular cylinders," *Journal of Fluid Mechanics*, vol. 70, no. 3, pp. 529–542, 1975.
- [22] E. Achenbach, "Influence of surface roughness on the cross-flow around a circular cylinder," *Journal of Fluid Mechanics*, vol. 46, no. Pt 2, pp. 321–335, 1971.

- [23] A. Fage and J. Warsap, "The effects of turbulence and surface roughness on the drag of a circular cylinder," *Aero. Res. Comm. R. & M.*, vol. 1283, 1929.
- [24] J. D. Guldsten, Personal Communication, 2010.
- [25] P. Weidman, "Wake transition and blockage effects on cylinder base pressures," 1968.
- [26] G. S. West and C. J. Apelt, "The effects of tunnel blockage and aspect ratio on the mean flow past a circular cylinder with reynolds numbers between 104 and 105," *Journal of Fluid Mechanics*, vol. 114, pp. 361–377, 2006.
- [27] M. J. Glanville and K. C. S. Kwok, "Further investigation of the blockage-tolerant wind tunnel technique," *Journal of Wind Engineering and Industrial Aerodynamics*, vol. 69, pp. 987–995, 1997.
- [28] K. G. Ranga Raju, O. P. S. Rana, G. L. Asawa, and A. S. N. Pillai, "Rational assessment of blockage effect in channel flow past smooth circular cylinders," *Journal of Hydraulic Research*, vol. 21, no. 4, pp. 289–302, 1983.
- [29] G. W. Jones, J. J. Cincotta, and R. W. Walker, "Aerodynamic forces on a stationary and oscillating circular cylinder at high reynolds numbers," *NASA-TR R-300*, 1969.
- [30] J. P. Batham, "Pressure distributions on circular cylinders at critical reynolds numbers," *Journal of Fluid Mechanics*, vol. 57, pp. 209–228, 1973.
- [31] A. Roshko, "Experiments on the flow past a circular cylinder at very high reynolds number," *Journal of Fluid Mechanics*, vol. 10, no. 3, pp. 345–356, 1961.
- [32] G. Schewe, "On the force fluctuations acting on a circular cylinder in crossflow from subcritical up to transcritical reynolds numbers," *J. Fluid Mech.*, vol. 133, pp. 265–285, 1983.
- [33] C. Farell and J. Arroyave, "On uniform flow around rough circular cylinders at critical reynolds numbers," *Journal of Wind Engineering and Industrial Aerodynamics*, vol. 36, pp. 621–631, 1990.
- [34] P. Bearman, "On vortex shedding from a circular cylinder in the critical reynolds number regime," *J. Fluid Mech.*, vol. 37, no. 3, pp. 577–585, 1969.
- [35] E. Achenbach, "Distribution of local pressure and skin friction around a circular cylinder in cross-flow up to  $Re=5 \cdot 10^6$ ," *Journal of Fluid Mechanics*, vol. 34, no. 4, pp. 625–639, 1968.
- [36] S. S. Diwan and O. N. Ramesh, "Laminar separation bubbles: Dynamics and control," *Sadhana*, vol. 32, no. 1, pp. 103–109, 2007.
- [37] O. U. Pfeil, H., "Boundary-layer transition on a cylinder with and without separation bubbles," *Experiments in Fluids*, vol. 10, no. 1, pp. 23–32, 1990.
- [38] Y. Han, B. Shi, X. Ren, and X. Jing, "Experimental study on the distribution of velocity and pressure near a submarine pipeline," *Journal of Ocean University of China (English Edition)*, vol. 8, no. 4, pp. 404–408, 2009.
- [39] B. Sumer and J. Fredsøe, *Hydrodynamics around cylindrical structures*, ser. Advanced Series on Ocean Engineering. World scientific, 1997, vol. 12.
- [40] A. Oner, M. Salih Kirkgoz, and M. Sami Akoz, "Interaction of a current with a circular cylinder near a rigid bed," *Ocean Engineering*, vol. 35, no. 14-15, pp. 1492–1504, 2008.
- [41] F. M. White, *Fluid Mechanics*, 5th ed. McGraw-Hill, New York, 2003.
- [42] G. Kaye and T. Laby, *Tables of physical and chemical constants*. Longman, 1995.